INFLUENCE OF CALCIUM ON GIBBSITE CRYSTALLIZATION: CALCIUM INCORPORATION WITHIN A GIBBSITE CRYSTAL LATTICE?

Haverty, D[1*], Raty, M[1], Stanton, KT[1, 2], Hodnett, BK[1] and Loan, M[1]
[1] *Materials and Surface Science Institute, University of Limerick, National Technological Park, Limerick, Ireland*
[2] *Department of Mechanical Engineering, University College Dublin, Belfield, Dublin, Ireland*

Abstract

The influence of calcium on the seeded crystallization of gibbsite was investigated using calcite in plant liquor at 65°C. Microscopy and de-supersaturation data demonstrates that calcium, as dissolving calcite, affects the processes of secondary nucleation and molecular growth, and as a result particle/crystal properties and the rate of crystallization. The data also suggests, that once available calcium is consumed a gibbsite crystal is able to recover through rapid defect growth, and that the affect of calcium on gibbsite crystal growth is also controlled by the rate of gibbsite precipitation. With the aid of molecular simulation and X-ray Photoelectron Spectroscopy (XPS) we tentatively postulate a possible mechanism of calcium action during gibbsite crystallization.

1 Introduction

In the Bayer process the addition of calcium as lime is widespread for a number of reasons (Burkin, 1987; Whittington, 1996; Chin, 1991; Solymar, 1993), being affectionately known as the 'aspirin' of the Bayer industry. Calcium is known to interact with gibbsite (Hind, 1999) affecting crystallization kinetics, morphology (Gnyra, 1976) and agglomeration (Brown, 1988). Industrially, calcium addition generally occurs in the form of 'lime' (CaO or $Ca(OH)_2$), but addition as calcium carbonate ($CaCO_3$) (Gnyra, 1976) and wollastonite ($CaSiO_3$) (Forte, 2004) has also been reported. Calcite in particular is added industrially as an aid during agglomeration. The solubility of calcium carbonate and its rate of equilibration have previously been investigated (Plummer, 1982; Raty, 2004), as has the solubility of lime (Rosenberg, 2001). Our previous studies of solubility equilibria (Raty, 2004) focused on using calcium to prevent gibbsite crystallization on red mud. The previous study considered calcium addition as the calcite polymorph of calcium carbonate, and we now present the next stages of this study here.

Lime ($Ca(OH)_2$) is very unstable in Bayer liquors and depending on the solution conditions (temperature, and caustic, aluminate and carbonate concentrations) will transform to a range of layered double hydroxides (in the nominal form of hydrocalumite – $[Ca_2Al(OH)_6]_2$• ½CO_2• OH• 5½H_2O) or tricalcium aluminate(s) (Rosenberg, 2001 & 2004; Buttery, 2004). Calcite, however, is more stable in Bayer liquors (with appreciable levels of carbonate), but can revert to hydrocalumite well below process temperatures (Buttery, 2004). For this reason, and because of its higher solubility compared to tricalcium aluminate (Rosenberg, 2001), calcite was chosen as the source of calcium in this study (Raty, 2004). $CaCl_2$ was not included due to the detrimental affect of chloride in Bayer liquors, and like $Ca(OH)_2$ and CaO, $CaCl_2$ is also unstable.

It is known from our previous work that calcium concentrations in solution decrease significantly in the presence of gibbsite, despite its lower surface area in comparison to other solids tested such as red mud (Raty, 2004). This indicates a clear affinity between calcium (as dissolving calcite) and the gibbsite surface. It is the intention of the present work to study this interaction during the crystallization of gibbsite. Particularly, if calcium levels decrease (Raty, 2004), where does it go? Is it incorporated into gibbsite or does it merely adsorb on the surface? Calcium compounds are known to be potent inhibitors of gibbsite crystallization and yet can improve agglomeration and agglomerate characteristics without affecting yield (Hind, 1999; Gnyra, 1976; Brown, 1988)? The mechanism whereby calcite influences the crystallization of gibbsite is not clear.

2 Experimental

Gibbsite seed was sourced from an alumina refinery (surface area, 0.2 m^2g^{-1}, median particle size (d_{50}), 60 µm, see Figure 1) and was exposed to a refinery grade calcite sample (Raty, 2004) in supersaturated plant liquor (A/C 0.6, C = 120 gL^{-1} as Na_2CO_3, Na_2CO_3 17 gL^{-1}). A seed charge of 5% was used in each crystallization experiment, with calcite added in concentrations of 0, 10 or 100 ppm. The solubility limit for calcium under these liquors is in the order of 10 ppm (Raty, 2004; Rosenberg, 2001). The undissolved solid phase acts as a reservoir of calcium ions, which continue to dissolve with Ca removal from solution due to its interaction with growing gibbsite crystals.

This explains why it is possible to dissolve 200 mgL^{-1} of $CaCO_3$ in seeded caustic alumina solution without formation of hydrated calcium aluminate phases (Gnyra, 1976).

Solutions were maintained at 65ºC for periods of up to 24 hours. Solids and filtered (0.45 µm) solutions were extracted during the course of experiments and then washed and dried prior to microscopy analyses. Aluminate solution concentrations (as g L^{-1} Al_2O_3) in similar solutions containing 0, 10 or 100 ppm Ca as above were measured using Inductively Coupled Plasma Spectroscopy (ICP).

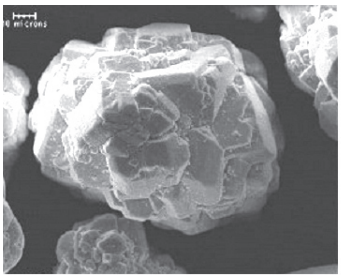

Figure 1: SEM image of the as received gibbsite seed

Scanning Electron Microscopy (SEM) analyses of samples were preformed on a JEOL JSM840 after coating with gold. Focused Ion Beam (FIB) milling and microscopy was carried out using an FEI Focused Ion Beam 200 instrument with a gallium ion source. To reduce charging effects the samples were also coated with gold prior to examination.

X-ray photoelectron (XPS) analyses were preformed in a Kratos Axis 165 spectrophotometer. The insulating samples were neutralized and the spectra calibrated using the C 1s binding position at 285 eV. Survey spectra were taken at low resolution between the binding energy

range of 1400 eV at 160 eV pass energy, 1 eV step size and 50 ms dwell time at each step. Then individual narrow range spectra for the elements of interest were acquired at high resolution with 20 eV pass energy, 0.05 eV step size and 100 ms dwell time. A monochromatic Al K_α (excitation energy: 1486.6 eV) at a voltage of 15 kV and current 5 mA was used. Samples were captured from solutions with 0, 10 and 100 ppm Ca added and examined for various crystallisation times.

Ab initio structure calculations were used to investigate possible Ca incorporation sites within the gibbsite lattice. All work was carried out within the Cerius2 modelling environment with the Cambridge Sequential Total Energy Package (CASTEP) used for *ab initio* superstructure Density Functional Theory (DFT) calculations (Accelrys, 2004). Geometry optimization was carried out at the Generalized Gradient Approximation (GGA) level with Vanderbilt ultra soft pseudopotentials to define the core states. A 4 k-point Monkhurst-Pack net and plane wave basis with a cut out energy of 750 eV to describe the valence electron density and the following convergence criteria were used: energy change = 2×10^{-5} eV per atom, rms force = 50 meV/Å per atom, rms displacement = 0.001 Å and rms stress = 0.1 GPa.

Two possibilities were investigated for Ca incorporation in the gibbsite lattice according to equation 1:

$$2Ca + Al_8(OH)_{24} \rightarrow Ca_2Al_8O_{24}H_2O + 2H_2 \quad (1)$$

These were the inter- and intra-layer sites in gibbsite, which until recently were also considered as possible sites for sodium incorporation (Vernon, 2005). H was determined for the above reaction to determine which site would be more thermodynamically favoured. It should be noted at this juncture that these calculations are exploratory in nature.

3 Results and Discussion

3.1 *Crystallization Experiments*

The results of the gibbsite crystallization experiments are shown in Table 1. The high supersaturation of 2.4, calculated using the Rosenberg and Healy model (1996), suggested secondary nucleation would dominate in these experiments. Analyses were focused on the early stages of precipitation and within the first hour the variation in aluminate concentrations were not significant. After two hours, however, Ca slowed the rate of crystallization, i.e. the development of an appreciable induction time with 100 ppm Ca, as has been documented previously (Gnyra, 1976; Brown, 1988). At 3 and 4 hours there was a significant difference between the 0 and 10 ppm Ca solutions indicating that Ca continues to affect the crystallization rate. Furthermore, this effect is transient as can be seen by the 24 hour values. Both the 0 and 10 ppm samples tended to similar equilibrium aluminate concentrations (despite the slower rate) while the 100 ppm sample continued to exhibit a retardation of the gibbsite crystallization rate, suggesting increased inhibition of surface growth sites. This was again similar to previous studies (Gnyra, 1976; Brown, 1988), and although the continued growth of gibbsite suggests a transient affect in these batch experiments, operation in a continuous and steady state process could occur with complete (i.e. transient) or incomplete consumption of calcite.

Table 1: Aluminate solution concentrations (as gL^{-1} Al_2O_3) as a function of time at each calcium concentration.

Time (hours)	0 ppm Ca	10 ppm Ca	100 ppm Ca
0	80.7	80.7	80.7
0.2	79.0	76.9	80.7
1	77.8	78.6	79.4
2	73.0	77.2	80.5
3	68.3	78.4	77.9
4	64.7	76.9	76.2
24	46.7	48.5	64.7

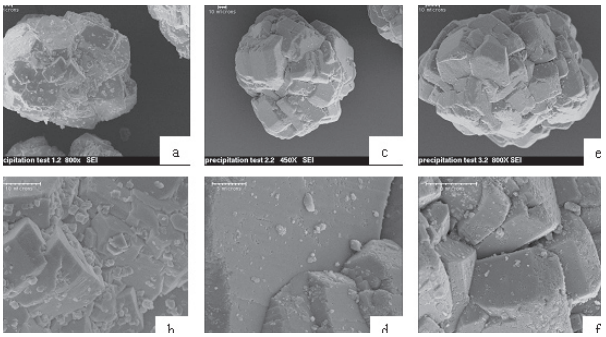

Figure 2: SEM images of gibbsite from crystallization experiments after 2 hours; low magnification (a, c and e), and higher magnification showing surface detail (b, d and f). O ppm Ca (a and b), 10 ppm Ca (c and d), and 100 ppm Ca (e and f).

SEM images of samples taken during crystallization experiments at various times with 0, 10 and 100 ppm Ca present are given in Figures 2–4.

There were clear differences between samples. In particular, calcium concentrations affect the processes of secondary nucleation and molecular growth. Figures 2–4 demonstrate that under the high supersaturation conditions used secondary nucleation is the dominant initial mechanism consuming available aluminate. However, the presence of increasing Ca concentrations inhibits secondary nucleation, reducing the number of nuclei and their crystalline character (i.e. absence of identifiable facets). It is this process which reduces the rate of crystallization in the 10 ppm Ca example, and increases the induction time in the 100 ppm case. Note, that although no calcium aluminate or hydrocalumite-type phases were identified within this study the relative proportion of such phases would be below the detection limit if present at all. We believe that the reported increase in agglomeration index (Gnyra, 1976; Brown, 1988) results from the inhibiting affect that Ca has on secondary nucleation (the absence of smaller secondary nuclei would give rise to larger a mean crystal size and hence agglomeration index).

Figures 2–4 also demonstrate that Ca affects molecular growth. Several images show what could be construed as pitting or etching of gibbsite surfaces. This indicates that there is a strong interaction between Ca and the gibbsite surface explaining why inhibition is more potent on the, higher surface area, smaller secondary nuclei. However, as de-supersaturation of the liquor continued we believe the observed roughening effect to be evidence of calcium inhibiting, but not preventing, molecular growth on the larger seed surfaces. The pitting arises as a result of localised molecular growth on the seed surface on regions bound by Ca. This is more obvious at longer times where growth of the seed surface is observed even in the presence of a high Ca concentration.

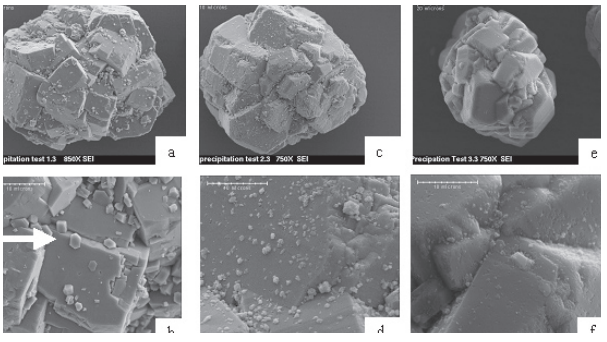

Figure 3: SEM images of gibbsite from crystallization experiments after 3 hours; low magnification (a, c and e), and higher magnification showing surface detail (b, d and f). O ppm Ca (a and b), 10 ppm Ca (c and d), and 100 ppm Ca (e and f). The arrow indicates a well-formed secondary nuclei crystal.

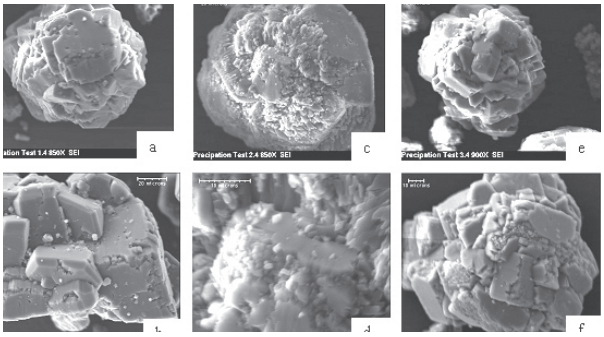

Figure 4: SEM images of gibbsite from crystallization experiments after 24 hours; low magnification (a, c and e), and higher magnification showing surface detail (b, d and f). O ppm Ca (a and b), 10 ppm Ca (c and d), and 100 ppm Ca (e and f).

At longer times and higher Ca concentrations the facet edges lose integrity, and the facets themselves also become roughened. It is possible that molecular growth within these defect regions will continue to occur until all the available Ca is consumed with the remaining supersaturation then results in more rapid growth perpendicular to the surface within the regions bound by these defect sites. These effects are more evident in the FIB images of Figure 5.

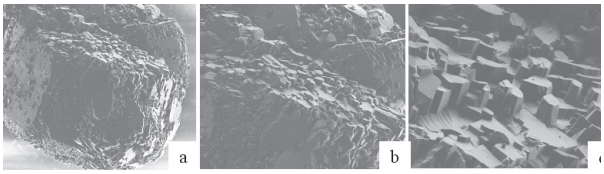

Figure 5: FIB image of a gibbsite sample from crystallization experiments after 24 hours in the presence of 100 ppm Ca, demonstrating a rapid growth affect from defect sites (increasing magnification a-c).

Secondary nuclei can grow and be incorporated into the lattice, or be removed from the growing surface by shear, crystal-crystal and crystal-crystallizer collisions. Hexagonal, rounded hexagonal, or lozenge (diamond-like) morphologies are conventionally thought to grow in preferred orientations from orientated surface defects; the variety of orientations helps facilitate agglomeration and surface healing through molecular growth.

The observation of the elongated features growing from the seed surface (Figure 5c) can be thought of as another secondary nucleation event, but in this case the initial nucleation and growth occurs on a smaller surface area bound by calcium containing sites. This causes crystals to grow rapidly in a vertical orientation, until they contact similarly constrained neighbouring growth regions to initialise agglomeration and the 'surface healing' observed in Figures 2–4. This demonstrates that although Ca inhibits crystallization its effect can be transient in nature. This also suggests a degree of structural homogeneity between the bulk gibbsite structure and any alternate surface structure with Ca. Hence the formation of an entirely different surface calcium aluminate phase such as tricalcium aluminate or hydrocalumite is unlikely. Calcium is more likely to act after the transport of growth units to the surface, and not act directly on species in solution (i.e. formation of a calcium aluminate species), which suggests the rate of precipitation and degree of available surface to be significant. Calcium also does not inhibit all the surface sites available for growth, as expected given the low levels used. The proposed action of gibbsite growth inhibition by Ca is summarised in Figure 6.

3.2 *X-ray Photoelectron Spectroscopy (XPS) and Modelling*

XPS results are shown in Figures 7–9. Although Ca was detected at minor levels in gibbsite surface layers throughout the course of all crystallization experiments, it is most apparent in the 100 ppm example (Figure 7). This XPS data indicates that Ca is concentrated at the surface or near surface layers of the precipitated material. The correlation between the O: Al atomic ratio (Figure 8) and the % Ca in the 100 ppm case suggests an increase in relative proportion of calcium to gibbsite (Figure 9). This complies with the previous interpretations from the crystallization experiments. The calcium concentration with respect to aluminium is shown in Figure 9. The Ca: Al ratio is typically less than 0.008, corresponding to 1 Ca in 15 unit cells, but reaches a maximum of 0.04 where the growth rate is slowest in the 100 ppm case, which implies 1 Ca in four unit cells.

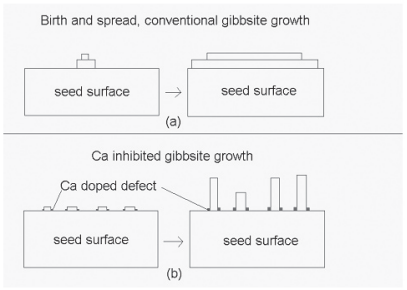

Figure 6: Schematic of the proposed mechanism of gibbsite growth inhibition by calcium.

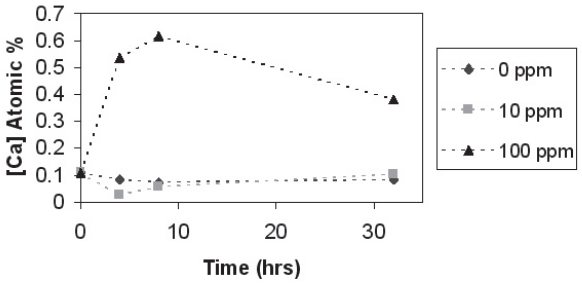

Figure 7: XPS data showing the atomic % of Ca in gibbsite surface layers as a function of time and Ca concentration.

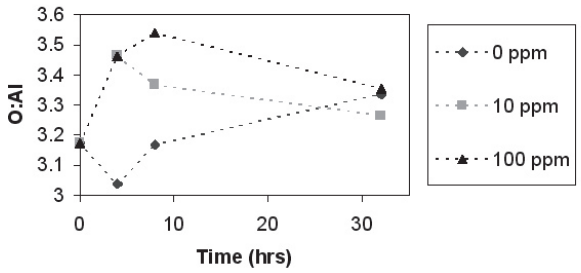

Figure 8: XPS data showing the O: Al atomic ratio in gibbsite surface layers as a function of time and Ca concentration.

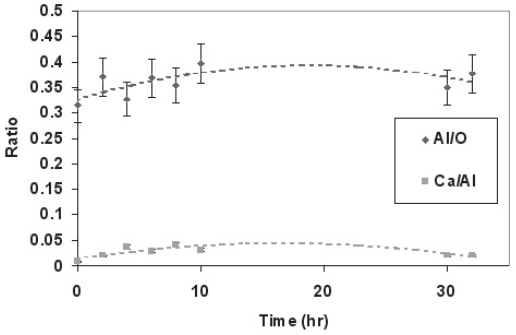

Figure 9: XPS data showing the atomic surface concentrations in the 100 ppm calcite sample as a function of time.

For further clarification and comparison, XPS data was also recorded for hydrocalumite and tricalcium aluminate (Figure 10). Figure 10 shows the calcium species in gibbsite surface layers are different to the similar

hydrocalumite and tricalcium aluminate surfaces. The Ca present in the gibbsite lattice is chemically distinct from the Ca in hydrocalumite and tricalcium aluminate, being more oxidised with the 2p core level occurring at a binding energy 0.46 eV higher. This suggests that Ca could be present in the gibbsite structure as Ca^{2+} ions and not as a separate Ca containing phase such as tricalcium aluminate or hydrocalumite.

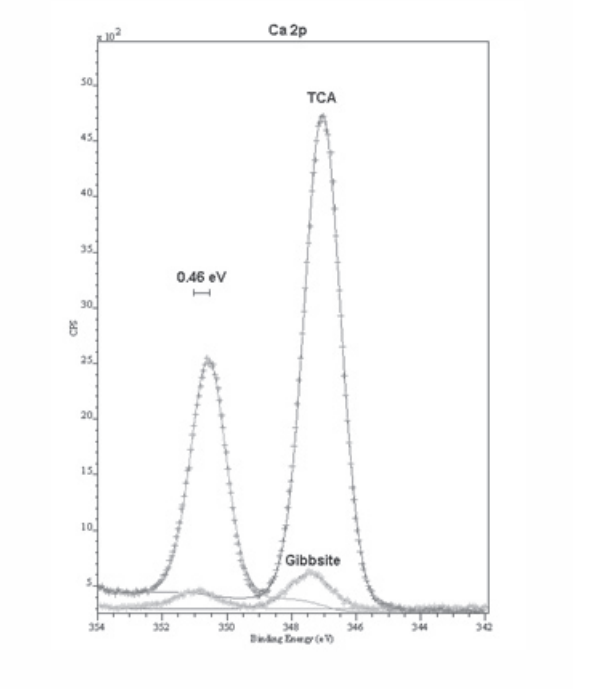

Figure 10: XPS data of gibbsite (100ppm calcium) and tricalcium aluminate (TCA), demonstrating the differences in calcium surface species.

Considering our hypothesis of possible structural homogeneity between the bulk gibbsite structure and any surface structure formed on addition of Ca, two simplistic and preliminary sites for calcium incorporation were considered. The gibbsite structure consists of pseudo-hexagonal pores formed by $Al(OH)_3$, where the layer plane is the pseudo basal plane. As gibbsite is also a layered structure, two possible sites for calcium could be within the inter-layer spacings or the hexagonal pores (i.e. intra-layer), which were until recently considered as sites for soda incorporation (Vernon, 2005). Enthalpy values for both the inter- and intra-layer sites were determined by ab initio calculations and are shown in Table 2. Structural schematics are shown in Figure 11.

Table 2: Lattice parameters, crystal symmetries and enthalpy values for both inter- and intra-layer site positions for Ca in the gibbsite lattice as determined using *ab initio* methods.

Site	a	B	c	β	Space group	ΔH (kJmol^{-1})
Gibbsite	8.68	5.08	9.74	94.54	P 21/c	
Intra-	8.94	5.15	9.41	93.07	P 21/c	–28.2
Inter-	8.71	5.07	9.55	95.83	P-1	–8.9

The enthalpy difference is greater for the intra-layer site. This suggests the most thermodynamically favoured site for calcium incorporation (absorption) within these two examples to be within the hexagonal pores of layer planes, and in this case without a large perturbation in the gibbsite structure (i.e. structural homogeneity). The structural homogeneity is also shown in Figure 11 and does not correspond to any of the calcium aluminate containing phases. It is therefore possible that although calcium may be able to pin surface growth sites, any preservation of structural homogeneity through Ca incorporation in growing gibbsite surface layers may permit the transient effect we observe during crystallization. This is despite the inhibitive impact on secondary nucleation and molecular growth.

Although the reactivity of calcium in Bayer liquors (Rosenberg, 2001 & 2004; Buttery, 2004) could be expected to produce surface calcium aluminate species, we believe the results from crystallization experiments, XPS and *ab initio* data suggest this to not be the case with calcite addition. Particularly, as formation of the structurally distinct phases of hydrocalumite, tricalcium aluminate, and even the postulated calcium aluminate monomer (Rosenberg, 2001), on the surface of gibbsite would not permit the transient effect of calcite that has been observed.

3.3 *Postulated Mechanism*

Several rate determining steps appear to be important to the dynamic mechanism of calcium action on a growing gibbsite crystal. The rates of calcium adsorption will be determined by the rates of calcite dissolution, which is controlled by the calcite solubility, and also the rate of gibbsite surface creation (i.e. growth and or secondary nucleation) providing new sites for calcium adsorption (i.e. calcium removal from solution). Hence, the rate of calcium removal from solution and also its efficiency in preventing secondary nucleation and inhibiting growth is not only controlled by the calcite concentration (i.e. how long the transient affect of calcium will last), but also the rate of precipitation (i.e. supersaturation and seed loading) and the surface area of available seed. Thus, the difference observed between this and previous studies with calcite (Gnyra, 1976; Brown, 1988).

At lower calcite concentrations the supply of calcium is insufficient to overcome the formation of secondary nuclei, but calcium rapidly adsorbs on higher area surfaces. Although a higher concentration of

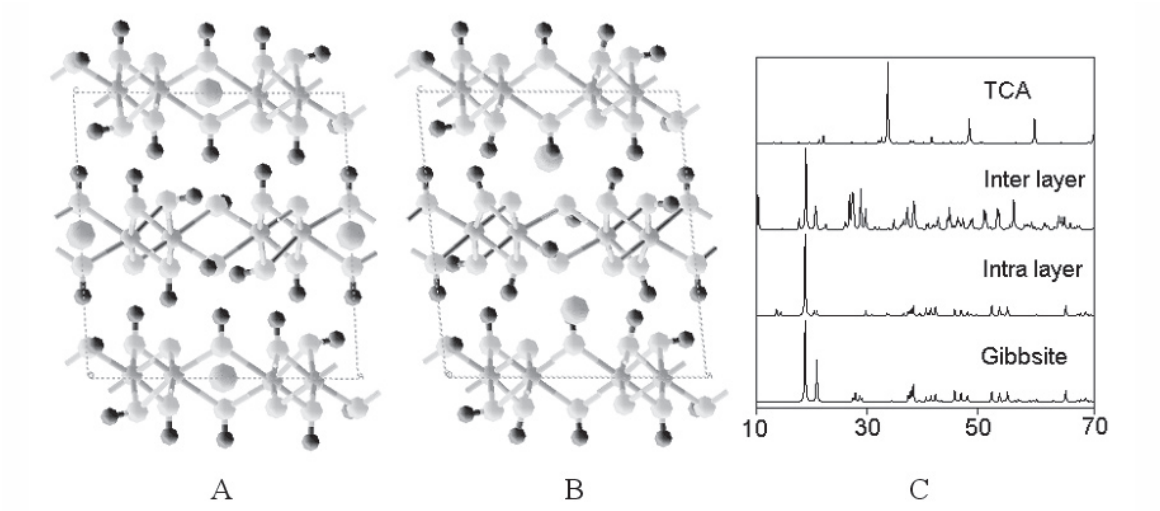

Figure 11: Structural schematics of possible intra- (A) and inter-layer (B) Ca sites in gibbsite. The calcium atoms are the larger spheres. (C) Comparison of Ca and aluminate containing crystal structure XRD patterns; tri-calcium aluminate (TCA), gibbsite and the inter- and intra-layer gibbsite models.

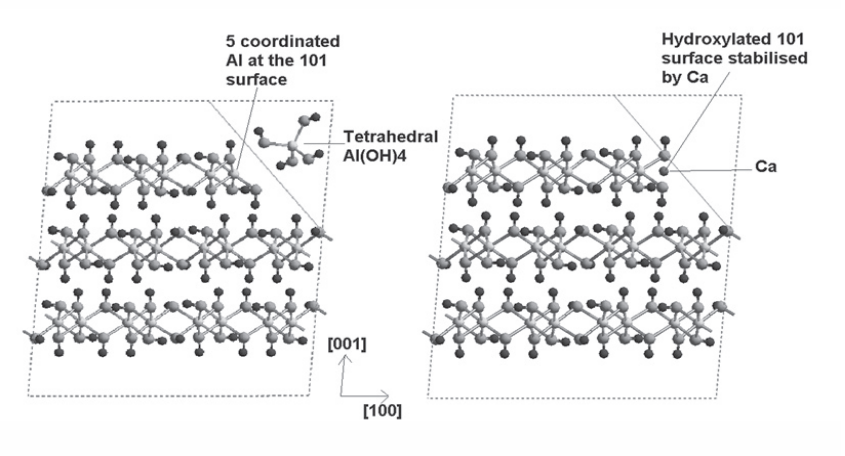

Figure 12: Postulated mechanism of molecular-scale calcium action, adsorption followed by absorption within a growing gibbsite crystal.

calcium prevents secondary nucleation, roughened growth of gibbsite occurs between pinned surface sites. After available calcium has been consumed, the rapid growth from defect sites occurs, with incorporation of calcium in structurally homogeneous sites and agglomeration regenerating a smooth gibbsite surface. This implies a mechanism of first adsorption of Ca^{2+} followed by incorporation (absorption), as depicted in Figure 12.

This mechanism implies the importance of further supersaturation and rate based experiments to delineate the influence of calcium on gibbsite crystallization. Further insight may also be gained through homogeneous precipitation of $Al(OH)_3$ with calcite, as the available volume in intra-layer sites is around 8% lower for the other polymorphs of gibbsite (calculated using Cerius2 software and a probe radius of 1.2 angstroms).

4 Conclusions

The effect of different concentrations of calcium ions on the crystallization of gibbsite under secondary nucleation conditions has been documented. Microscopy and de-supersaturation data demonstrated that calcium as dissolving calcite affects the processes of secondary nucleation and molecular growth, reducing the rate of crystallization, primarily by preventing secondary nucleation in this case. The low solubility of calcium in solution does, however, not affect its efficacy. We believe that the previous reports of increase in agglomeration index relate to the inhibition of traditional secondary nucleation mechanisms, which can involve increased attrition. The transient impact of calcium we have documented relates to its dynamic consumption (i.e. continued dissolution of residual calcite) by growing gibbsite, until supersaturation promotes a rapid defect growth affect that eventually involves surface healing. Through preliminary molecular simulation and X-ray Photoelectron Spectroscopy (XPS) data we tentatively postulate that such a process is viable due to a level of structural homogeneity being retained after calcium incorporation within intra-layer sites of gibbsite.

Acknowledgements

Aughinish Alumina Ltd is thanked for financial support. M. Mihov and D. Sutton are thanked for the FIB images.

References

Brown, N. (1988) Effect of calcium ions on agglomeration of Bayer aluminium trihydroxide. Journal of Crystal Growth, 92:26–32.

Burkin, A.R. (1987) Production of Alumina and Aluminium, volume 20 of Critical Reports on Applied Chemistry. John Wiley and Sons, New York.

Buttery, J.H.N., Patrick, V.A., Rosenberg, S.P., Heath, C.A. and Wilson, D.J. (2002) Thermodynamics of hydrocalumite formation in cauticisation. Light Metals, p 185–190.

Forte, G. (2004) Wollastonite as a substitute for lime in phosphorous control during digestion and as a precoat or filter aid for pregnant liquor filtration in the Bayer process. Light Metals, p 5–7.

Gnyra, B. & Brown, N. (1976) The coarsening of alumina trihydrate by means of crystallization modifiers. Powder Technology, 11:101–105.

Hind, A.R., Bhargava, S.K. and Grocott, S.C. (1999) The surface chemistry of Bayer process solids: a review. Colloids and Surfaces A: Physicochemical and Engineering Aspects, 146:359–374.

Konno, H., Nanri, Y. and Kitamura, M. (2002) Crystallization of aragonite in the causticizing reaction. Powder Technology, 123:33–39.

MS CASTEP Datasheet. www.accelrys.com, September 2004.

Plummer, L. and Busenburg, E. (1982) The solubilities of calcite, aragonite and vaterite in $CO_2 - H_2O$ solutions between 0 and 90°C and an evaluation of the aqueous model for the system $CaCO_3 - CO_2 - H_2O$. Geochimica et Cosmochimica Acta, 46:1011–1040.

Raty, M., Stanton, K.T., Hodnett, B.K. and Loan, M. (2004) Calcite in the mud washing circuit of the Bayer process: Experimental solubility and adsorption. Light Metals, p 105–108.

Rosenberg, S.P. and Armstrong, L. (2005) Layered Double hydroxides in the Bayer process: Past, present and future. Light metals, pp 157–161.

Rosenberg, S.P. and Healy, S.J. (1996) A thermodynamic model for gibbsite solubility in Bayer liquor. Proceedings of the Fourth Alumina Quality Workshop, Darwin Australia, p 301–310.

Rosenberg, S.P., Wilson, D.J. and Heath, C.A. (2001) Some aspects of calcium chemistry in the Bayer process. Light Metals, pp 19–25.

Solymar K. and Zoldi, J. (1993) Lime in the Bayer process: present state and future trends. Light Metals, pp 185–193.

Vernon, C., Loh, J., Lau, D. and Stanley, A. (2005) Soda incorporation during hydrate precipitation. Light Metals, pp 190–196.

Whittington, B. (1996) The chemistry of CaO and $Ca(OH)_2$ relating to the Bayer process. Hydrometallurgy, 43:13–35.

Chin, L.A.D. (1991) Chemical additives in the Bayer process. Light Metals, pp 155–158.